*Human Molecular Genetics, 2011, Vol. 20, No. 15* **3067–3078**
*doi:10.1093/hmg/ddr210*
*Advance Access published on May 10, 2011*

# MicroRNA profiling of Parkinson's disease brains identifies early downregulation of miR-34b/c which modulate mitochondrial function

**Elena Miñones-Moyano[1,2,†], Sílvia Porta[1,3,†], Georgia Escaramís[1], Raquel Rabionet[1], Susana Iraola[1], Birgit Kagerbauer[1], Yolanda Espinosa-Parrilla[4], Isidre Ferrer[3,6], Xavier Estivill[1,5,*] and Eulàlia Martí[1,*]**

[1]Genetic Causes of Disease Group, Genes and Disease Program, Centre for Genomic Regulation (CRG), Barcelona, Catalonia, Spain, [2]Universitat de Barcelona, Barcelona, Catalonia, Spain, [3]Institut de Neuropatologia, Servei Anatomia Patològica, IDIBELL-Hospital Universitari de Bellvitge, Universitat de Barcelona, Barcelona, Catalonia, Spain, [4]IBE, Institute of Evolutionary Biology (UPF-CSIC), CEXS-UPF-PRBB, Barcelona, Catalonia, Spain, [5]Experimental and Health Sciences Department, Pompeu Fabra University, Barcelona, Catalonia, Spain and [6]Centro de Investigación Biomédica en Red sobre Enfermedades Neurodegenerativas (CIBERNED), Instituto Carlos III, Spain

Received February 2, 2011; Revised April 29, 2011; Accepted May 5, 2011

**MicroRNAs (miRNAs) are post-transcriptional gene expression regulators, playing key roles in neuronal development, plasticity and disease. Parkinson's disease (PD) is the second most common neurodegenerative disorder, characterized by the presence of protein inclusions or Lewy bodies and a progressive loss of dopaminergic neurons in the midbrain. Here, we have evaluated miRNA expression deregulation in PD brain samples. MiRNA expression profiling revealed decreased expression of miR-34b and miR-34c in brain areas with variable neuropathological affectation at clinical (motor) stages (Braak stages 4 and 5) of the disease, including the amygdala, frontal cortex, substantia nigra and cerebellum. Furthermore, misregulation of miR-34b/c was detected in pre-motor stages (stages 1–3) of the disease, and thus in cases that did not receive any PD-related treatment during life. Depletion of miR-34b or miR-34c in differentiated SH-SY5Y dopaminergic neuronal cells resulted in a moderate reduction in cell viability that was accompanied by altered mitochondrial function and dynamics, oxidative stress and reduction in total cellular adenosin triphosphate content. MiR-34b/c downregulation was coupled to a decrease in the expression of DJ1 and Parkin, two proteins associated to familial forms of PD that also have a role in idiopathic cases. Accordingly, DJ1 and Parkin expression was reduced in PD brain samples displaying strong miR-34b/c downregulation. We propose that early deregulation of miR-34b/c in PD triggers downstream transcriptome alterations underlying mitochondrial dysfunction and oxidative stress, which ultimately compromise cell viability. A better understanding of the cellular pathways controlling and/or controlled by miR-34b/c should allow identification of targets for development of therapeutic approaches.**

## INTRODUCTION

Parkinson's disease (PD) is the second most common neurodegenerative disease, affecting 1–2% of the population over 60 years old (1,2). PD is clinically characterized by motor symptoms as resting tremor, slowness of initial movement, rigidity and general postural instability. The disease is pathologically defined by the loss of dopaminergic neurons in the substantia nigra (SN) pars compacta, corpus striatum and brain cortex. This loss is accompanied by the presence of cytoplasmic protein inclusions, named Lewy bodies (LBs), and enlarged aberrant Lewy neurites (LNs) (3–5). For this

*To whom correspondence should be addressed. Email: eulalia.marti@crg.cat (E.M.); xavier.estivill@crg.cat (X.E.)
†E.M.-M. and S.P. are equal first contributing authors.

reason, PD is known as a Lewy body disease (LBD). LBs and LNs are composed of aggregates of normal and missfolded proteins, being α-synuclein (SNCA) a major component. The intracerebral formation of LBs and LNs has been proposed to begin at defined induction sites and advance in a topographically predictable sequence, defining six evolutionary stages, according to Braak *et al*. (3,4). Lesions are first observed in the medulla oblongata (stages 1–2), then the midbrain and amygdala (AM) (stages 3–4) and finally the cerebral cortex (stages 5–6). Motor symptoms appear when neuron loss in the substantia nigra (SN) pars compacta reaches thresholds values near the 60% at late stage 3 or at stage 4. Cases with Lewy pathology in the brain stem without clinical evidence of parkinsonism are considered pre-motor PD or incidental LBD (6,7).

Genetic studies show that mutations in *SNCA*, *PARKIN*, *UCHL-1*, *PINK1*, *DJ-1* and *LRKK2* are the origin of familial cases of PD, although they account only for 5–10% of patients. The majority of PD cases are idiopathic (2,8–10). Although familial and idiopathic forms of the disease differ on several clinical aspects, it is clear that common molecular pathways underlie neurodegeneration. These include oxidative stress, mitochondrial dysfunction, energy production imbalance and disruption of the ubiquitin–proteasome system. The study of these pathways has shed some light on the mechanisms underlying PD, but the causative factors for idiopathic PD remain elusive.

MicroRNAs (miRNAs) are small non-coding RNAs that have been recently identified as post-transcriptional regulators of gene expression with relevant roles in physiological and pathological aspects of the central nervous system (11,12). MiRNAs conduct targeted-mRNA degradation or translational inhibition through sequence complementarity to the open reading frames and 3′ untranslated regions (3′UTR) of mRNAs (13,14). Alterations in miRNA function have been reported in a number of neurodegenerative diseases (15). In PD, abnormal function of three miRNAs has been shown. For instance, the expression of miR-133b, a miRNA essential in the differentiation and maintenance of dopaminergic neurons in the SN, was reduced in midbrain samples from patients with PD (16). In addition, disruption of the binding site for miR-433 in the *FGF20* gene has been associated to PD, and *FGF20* over-expression has been shown to correlate with higher *SNCA* expression levels (17). Finally, miR-7 was shown to be downregulated in a PD mouse model (18). This study further demonstrated that miR-7 expression reduces SNCA levels, resulting in cell protection from oxidative stress. Although these findings suggest an involvement of miRNAs in PD, a general screening of miRNA expression deregulation in the brain of PD patients is still lacking.

Here, we have evaluated miRNA deregulation in differently affected brain areas from idiopathic PD patients at different evolutionary stages of the disease. With this study, we aim to uncover deregulation of gene expression networks affecting key pathogenic pathways in sporadic PD. Our study has identified that miR-34b/c downregulation is widespread in PD brains, occurring early in the course of the disease, and underlying mitochondrial dysfunction and oxidative stress.

## RESULTS

### miR-34b/c cluster is downregulated at advanced stages of PD

In a first attempt to identify miRNAs with a possible role in PD, we focused on motor stages of the disease (stages 4 and 5). The initial screening was performed in the AM. We profiled miRNA expression in PD using a commercial miRCURY™ array (Exiqon) that contained all miRNAs present in the miRBase miRNA registry release 8.1. Expression patterns of miRNAs in the AM of 11 PD patients were compared with those of a pool of samples formed by equivalent amounts of total RNA of the AM of six control individuals without neuropathological lesions (Supplementary Material, Table S1). Two miRNAs (miR-637 and miR-34c-5p) were downregulated by >40% in 9 out of the 11 PD samples, compared with the control pool (Supplementary Material, Fig. S1). The microarray results were further evaluated using real time polimerase chain reaction (RT–PCR) Taqman® assays. While we were not able to confirm the deregulation of miR-637, RT–PCR analysis corroborated significant downregulation of miR-34c in the AM of PD patients. Results were similar either using U6B or RNU58 as reference small non-coding RNAs (Supplementary Material, Fig. S1).

MiR-34c and miR-34b are located 411 bp apart on chromosome 11q23 and are transcribed as a single non-coding precursor. Therefore, we evaluated the expression of both mature miRNAs in additional symptomatic PD and control AM samples (Supplementary Material, Table S1). PD–AM displayed a significant decrease in the expression of mir-34b and mir-34c by ∼55 and 65%, respectively, versus control individuals (Fig. 1A). The expression of miR-34b and miR-34c was also reduced in the SN of PD patients by 40 and 45%, respectively (Fig. 1B). However, whether the decreased expression is a consequence of dopaminergic neuron depletion in this area or is a specific downregulation in the remaining cells remains to be resolved. We then determined if miR-34b/c downregulation in motor PD cases was extensive to other areas of the brain with different degree of neuropathological affectation. We detected a significant reduction (∼55%) in both miR-34b and miR-34c in the frontal cortex (FC), an area with absent or scanty LBS and LNs depending on the stage but with well-established molecular deficits (8) (Fig. 1C). Additionally, the cerebellum (CB), a structure with virtually no lesions in PD, presented a less robust downregulation of miR-34b (∼23%) showing a trend to significance ($P = 0.056$), and a significant downregulation of miR-34c (∼43%) (Fig. 1D).

The differences in the degree of miR-34b and miR-34c downregulation may be related with a possible differential stability of mature miRNAs in the different areas. To test this, we determined the relative expression of miR-34c versus miR-34b within each area in control individuals (Supplementary Material, Fig. S2 and Table S1). Although the amount of miR-34c was significantly higher compared with miR-34b in the AM, the rest of areas analyzed showed similar levels of both miRNAs. These results suggest region-dependent mechanisms controlling the expression and/or stability of miR-34c and miR-34b. The fact that the relative levels of miR-34c versus miR-34b change in diseased AM and CB

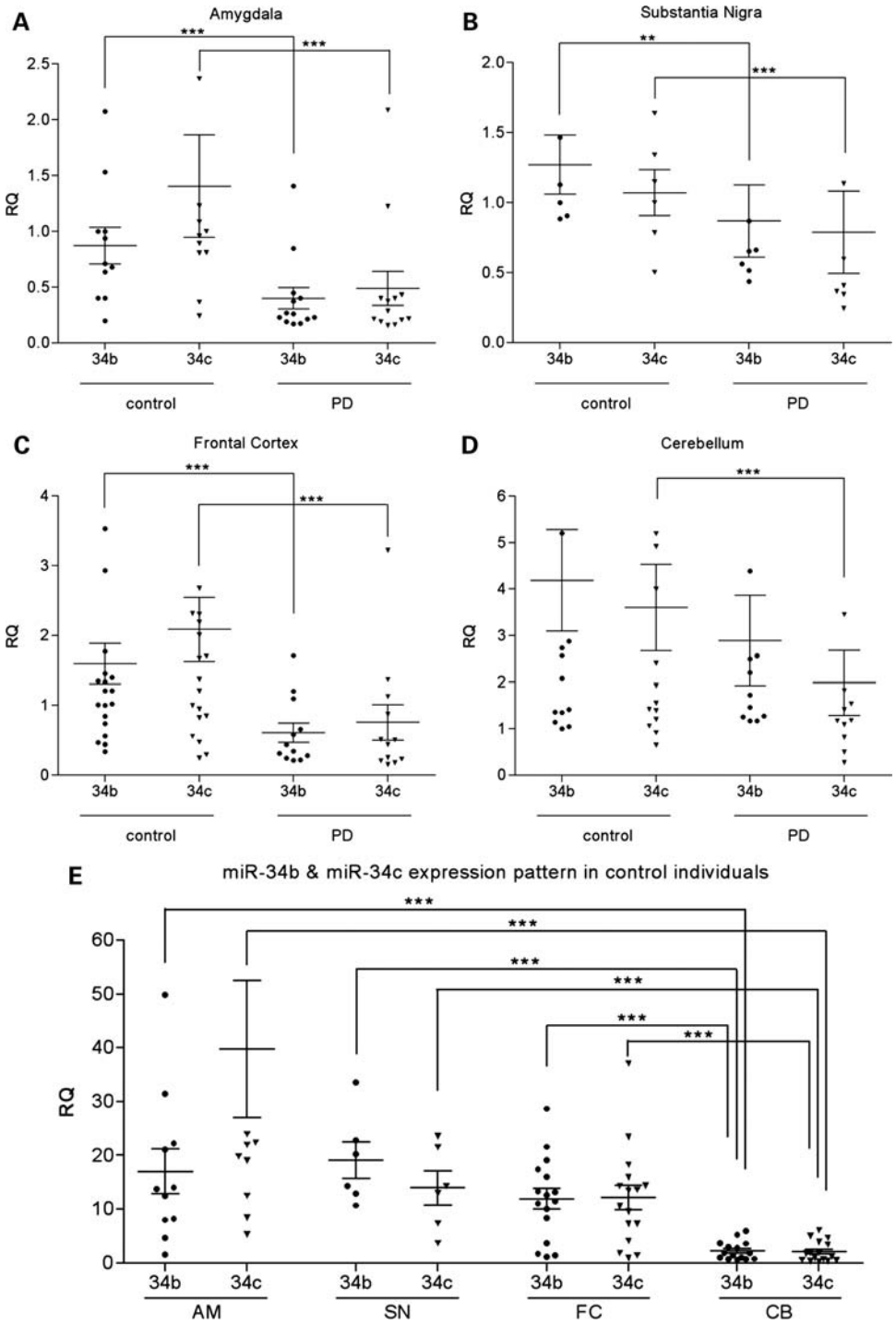


**Figure 1.** miR-34b and miR-34c expression in different brain regions from PD cases stages 4 and 5 (motor stages of PD). (**A**–**D**) miR-34b and miR-34c levels are shown in control individuals and motor PD cases (listed in Supplementary Material, Table S1) in the AM (A), SN (B), FC (C) and CB (D). MiR-34b and miR-34c expression levels are referred to a control sample, for RQ. (**E**) MiR-34b and miR-34c expression levels in the AM, SN, FC and CB of control individuals. The CB is used as the reference area, for RQ. Plots show individual and mean RQ ± SEM ($^{*}P < 0.05$; $^{**}P < 0.01$; $^{***}P < 0.001$; using a linear mixed effects model).

suggests that these mechanisms are also dependent on the pathological state.

Areas showing high expression of miR-34b/c under normal conditions may probably be more susceptible to the downstream consequences of miR-34b/c decrease. In order to evaluate the importance of the area-dependent miRNA-34b/c downregulation, we determined the levels of miR-34b/c in the different brain areas in control individuals. The CB contained the lowest levels of miR-34b/c when compared with the rest of brain areas (Fig. 1E and Supplementary Material, Fig. S3 and

Table S1). The lower levels of miR-34b/c in the CB and the observed moderate downregulation support the idea that miR-34b/c decrease has lower pathological consequences in this area when compared with other brain regions.

Downregulation of miR-34b/c has been associated with hypermethylation of the neighboring CpG islands in the promoter region in colorectal cancer (19). Therefore, we analyzed the methylation status of the described promoter region in the AM from six selected PD cases that presented clear miR-34b/c downregulation compared with the controls, and from three controls (Supplementary Material, Table S1). Bisulfite sequencing showed low methylation levels in all samples independently of the mir34b/c expression levels (Supplementary Material, Fig. S4). These low methylation levels of the promoter are in accordance with those obtained in an independent study on various brain tissues from PD and control samples using a methylation array (Illumina Infinium 27K) (Raquel Rabionet, personal communication).

### miR-34b/c downregulation is an early event in PD that is not related to drug therapies

In order to assess if miR-34b/c downregulation correlated with the evolution of the disease, we evaluated the expression of these miRNAs in the AM and FC of PD cases at pre-motor stages (Braak stages 1–3; Supplementary Material, Table S1). We observed a significant reduction in the expression of both miR-34b and miR-34c of 35 and 45%, respectively, in the AM of pre-motor cases compared with control samples (Fig. 2A). However, the decrease in miR-34b/c expression in the FC of PD pre-motor cases did not reach statistical significance (Fig. 2B). It is important to state that none of the patients bearing neuropathological changes of PD-related pathology stages 1–3 received any treatment related to PD; as these cases had not suffered from motor symptoms and pathological findings were, by definition, as incidental in the course of the neuropathological examination.

### miR-34b and miR-34c reduction compromises neuronal viability by mitochondrial dysfunction and reactive oxygen species production

Mitochondrial dysfunction linked to oxidative stress is a relevant feature in neurodegenerative processes, including PD. Therefore, we evaluated cell viability linked to mitochondrial functional status following miR-34b or miR-34c depletion in the differentiated SH-SY5Y dopaminergic neuroblastoma cell line.

SH-SY5Y cells were differentiated with retinoic acid (RA) and 12-O-tetradecanoyl-phorbol-13-acetate (TPA) to a postmitotic status, exhibiting a dopaminergic phenotype (20). The differentiation process was associated to a significant 2-fold rise in the expression levels of miR-34b and miR-34c (Supplementary Material, Fig. S5), suggesting a relevant role of these miRNAs in the physiology of postmitotic mature neurons. Differentiated SH-SY5Y cells were transfected either with specific inhibitors for miR-34b or miR-34c or a scrambled sequence inhibitor (Dharmacon), and cell viability was determined at different time points post-transfection, using the 3-(4,5-dimethylthiazol-2-yl)-2,5-diphenyltetrazolium bromide (MTT) assay. Transfection with the inhibitors resulted in a decrease in endogenous miR-34b and miR-34c expression by 60–70% approximately (Supplementary Material, Fig. S6), which is comparable to the downregulation observed in PD brain samples. We detected a consistent decreased capability of mitochondria to reduce MTT at 24, 48 and 72 h after miR-34b or miR-34c depletion, compared with the control group transfected with the scrambled sequence (Fig. 3A). These results were reproduced using LNA-modified miRNA inhibitors (Exiqon) (Supplementary Material, Fig. S7).

Mitochondrial dysfunction was confirmed using the MitoTracker® Red CMXRos (Invitrogen) fluorescent dye that stains mitochondria in live cells, being its accumulation dependent on membrane potential. Mitotracker® Red revealed a strong tubular mitochondrial staining throughout the cytoplasm in control non-transfected cells and neuronal cells transfected with a scrambled sequence. However, 24 and 48 h after transfection with anti-miR-34b or anti-miR-34c a significant increase of the number of cells displaying a uniform, dissipate mitochondrial staining was observed (Fig. 3B). We next evaluated whether the disruption of mitochondrial membrane potential was coupled to altered expression of proteins of the electron transport chain. For this, we used the MitoProfile® Total OXPHOS, OXPHOS cocktail of monoclonal antibodies (MitoSciences) against subunits of mitochondrial complexes that are labile when its complex is not assembled. Western blot analysis showed no differences in the expression levels of the subunit 30 kDa (complex II), subunit Core 2 (complex III), subunit II (complex IV) and subunit alpha (adenosin triphosphate (ATP) synthase) at 48 and 72 h post-transfection of the specific inhibitors for miR-34b or miR-34c (Supplementary Material, Fig. S8).

We then tested if the decrease in neuronal viability induced by miR-34b or miR-34c depletion was linked to the generation of intracellular reactive oxygen species (ROS), using the cytosolic fluorescence probe, 5-(and-6)-chloromethyl-2′-7′- dichlorodihydrofluorescein diacetate (CM-H2DCFDA, Invitrogen). The redox-sensitive probe was able to perceptively detect oxidative stress 24 h after transfection with anti-miR-34b or anti-miR34c, whereas virtually no fluorescence was detected in cells transfected with a scrambled sequence (Fig. 3C).

To further characterize neuronal dysfunction, we evaluated cytochrome-c mobilization from the mitochondria to the cytoplasm, since this can be a distinctive feature of the early pro-apoptotic stimuli linked to the loss of mitochondrial membrane potential. Immunofluorescence showed no cytochrome-c release 24 and 48 h after transfection with anti-miR-34b or anti-miR-34c (Fig. 4A), suggesting a non-apoptotic mechanism. In accordance, at these time points, the decrease in cell viability was not accompanied by significant nuclear condensation or fragmentation (Figs 3B–C and 4A), or increases in PARP cleavage as evaluated by western blot (data not shown). Importantly, cytochrome-c immunostaining revealed a ballooning of the mitochondria following miR-34b or miR-34c depletion (Fig. 4A, arrows in the upper panel). Ultrastructural analysis of mitochondria in SH-SY5Y depleted of miR-34b confirmed the presence of ballooned small mitochondria (Fig. 4B).

In order to correlate the abnormal mitochondrial morphology and loss of membrane potential with a functional defect, we analyzed the intracellular levels of ATP following miR-34b and miR-34c depletion (Fig. 4C). Bioluminiscent

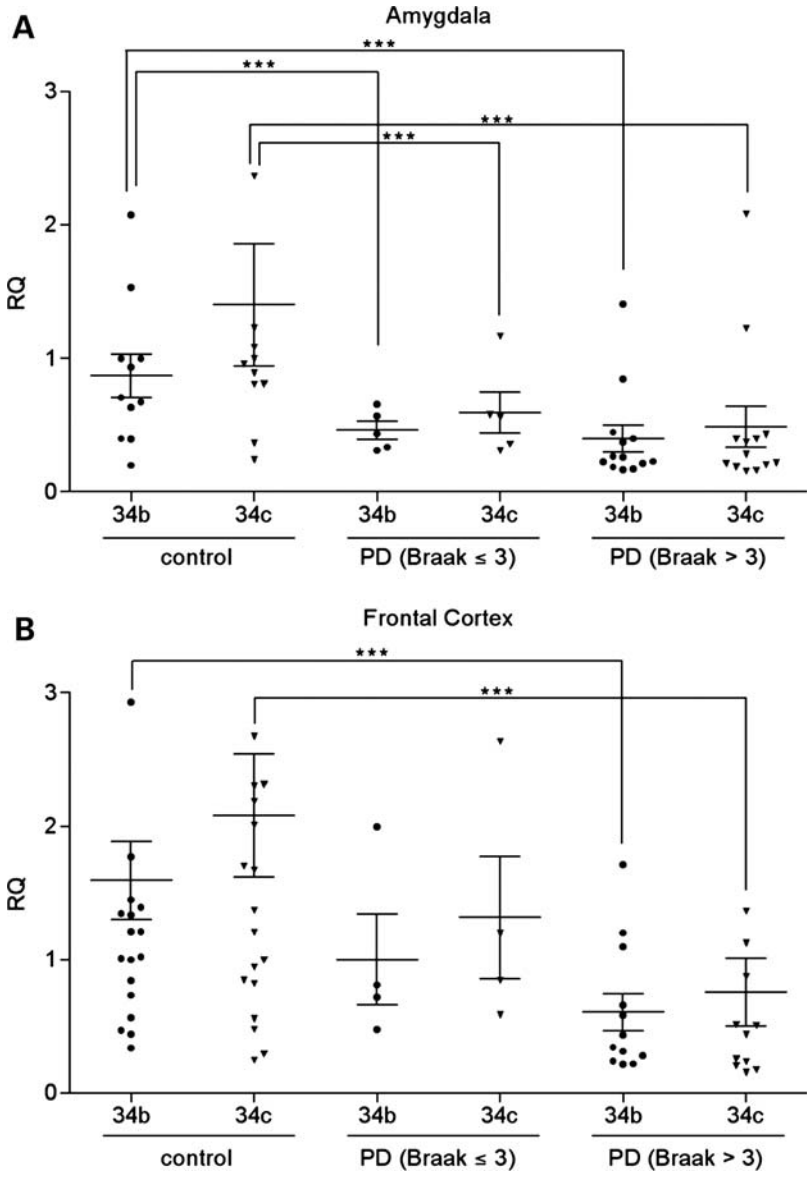


**Figure 2.** miR-34b and miR-34c expression in brain samples of pre-motor PD cases (stages 1–3). MiR-34b and miR-34c expression levels in control, pre-motor PD (stages 1, 2 and 3) and clinical PD (stages 4 and 5) in the AM (**A**) and FC (**B**) (listed in Supplementary Material, 1 Table S1). Expression levels are referred to a control sample, for RQ. Plots show individual and mean RQ ± SEM ($^{*}P < 0.05$; $^{**}P < 0.01$; $^{***}P < 0.001$; using a linear mixed effects model).

measurements of intracellular ATP evidenced a significant decrease in the ATP content 48 h after anti-miR-34b or anti-miR-34c transfection. Taken together, these results suggest that miR-34b and miR-34c are involved in pathways controlling mitochondrial function and dynamics, and their depletion may trigger a non-apoptotic deleterious process achieved by mitochondrial dysfunction.

We determined whether the decrease in cell viability and mitochondrial dysfunction linked to miR-34b/c downregulation could also be detected in non-differentiated SH-SY5Y cells and two non-neuronal cell lines (RPE-1 epithelial retinal cells and HepG2 hepatocellular carcinome cells; Supplementary Material, Fig. S9). A slight decrease in neuronal viability was observed in non-differentiated SH-SY5Y cells depleted of miR-34c and in hepG2 cells depleted of miR-34b. However, in these cells, no obvious changes in mitochondrial function and morphology were appreciated. A possible explanation for this is that the levels of miR-34b/c in the different cells lines, including the non-differentiated neuronal type, are low, and therefore its inhibition may not be physiologically relevant, compared with the differentiated neuronal cells that present higher levels of miR-34b/c. In addition, it is also plausible that the interaction of miR-34b/c with components of the differentiated neuronal transcriptome may result in selective, increased affectation.

### miR-34b or miR-34c reduction results in a decreased expression of DJ1 and PARKIN

*DJ1*, *PARKIN* and *PINK1* are among the group of genes associated to familial forms of PD that have a direct or indirect impact on oxidative stress balance and mitochondrial integrity

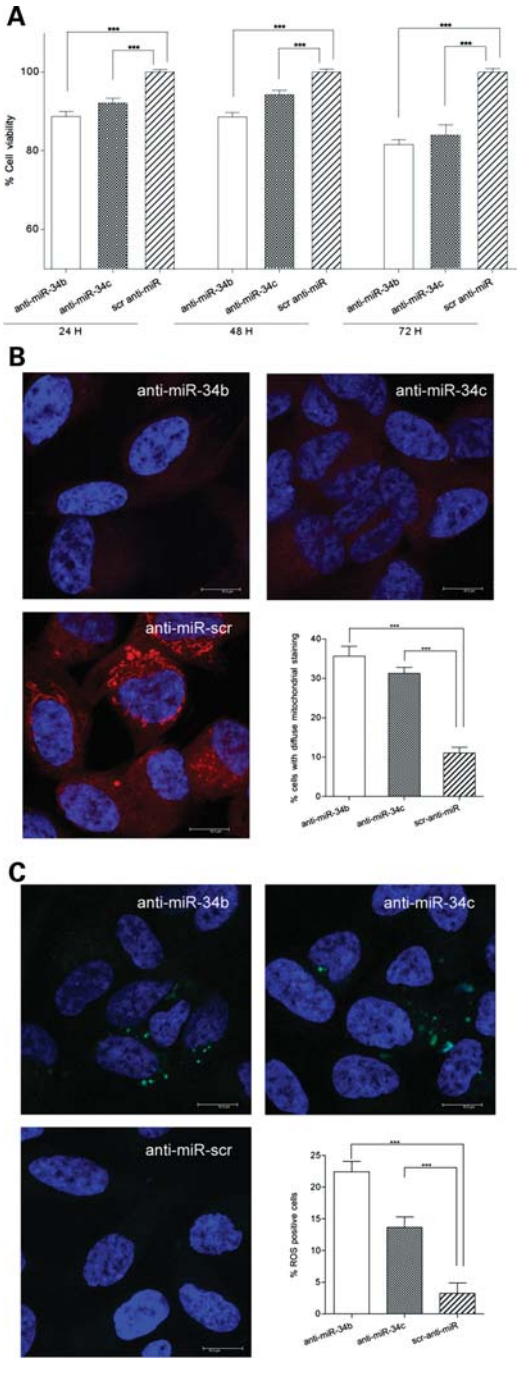


**Figure 3.** Analysis of cell viability, mitochondrial function and oxidative stress after miR-34b or miR-34c depletion. (**A**) MTT assays at 24, 48 and 72 h after transfection of SH-SY5Y cells with inhibitors to miR-34b (anti-miR-34b), miR-34c (anti-miR-34c) or a scramble sequence (scr-anti-miR). Data represent mean basal viability ± SEM ($n = 12$; $^{***}P < 0.001$, using $t$-test). (**B**) Mitochondrial labeling with red fluorescent MitoTracker® Red and DAPI staining of differentiated SH-SY5Y cells 24 h after transfection of either miR-34b or miR-34c inhibitors or a scrambled-control sequence; graph shows the mean percentage of cells presenting diffuse staining ± SEM ($n = 3$; ***, $P < 0.001$; using $t$-test). (**C**) ROS detection with green fluorescent probe CM-H2-DCFDA and DAPI staining of differentiated SH-SY5Y cells 24 h after transfection of either miR-34b or miR-34c inhibitors or a scrambled sequence. The graph shows the mean percentage of cells positive for ROS detection ± SEM ($n = 3$; $^{***}P < 0.001$; using $t$-test).

and function (21). The expression levels of these non-mutated proteins have been shown to modify the cell response to oxidative stress (22,23); consequently, they could have a role in idiopathic forms of the disease. We therefore evaluated the effect of miR-34b or miR-34c depletion in the expression of these proteins by western blot (Fig. 5A–C). We detected a significant reduction in DJ1 and Parkin levels upon miR-34b and miR-34c depletion at 48 h post-transfection. However, no significant changes on PINK1 levels were observed. In addition, overexpression of miR-34b or miR-34c in transfection experiments using miRIDIAN miRNA mimics (Ambion) did not result in changes in the expression of Parkin or DJ-1 (data not shown). Although recent databases on predicted miRNA targets (miRWalk; http://www.ma.uni-heidelberg.de/apps/zmf/mirwalk/index.html) identify Parkin as a candidate target of miR-34b, our data suggest that Parkin and DJ-1 are indirect targets of miR-34b/c.

We next examined whether the expression levels of DJ1 and Parkin were also reduced in brain samples from PD patients. Protein levels were determined in the AM and FC of four control individuals and four PD patients, which presented strong miR-34b/c downregulation (Supplementary Material, Tables S1 and S2). Western blot analysis revealed a significant decrease in the expression of DJ1 and Parkin in AM samples of PD patients compared with control individuals. In the FC, DJ1 and Parkin protein expression was variable and reduced levels were detected for both proteins in PD samples; however, they did not reach statistical significance (Fig. 5D–E). These findings suggest that mitochondrial dysfunction linked to miR-34b/c downregulation may involve, at least in part, a decreased expression of DJ1 and Parkin.

## DISCUSSION

miRNA deregulation in neurodegenerative disorders underlies altered expression of key target genes, contributing to neuronal dysfunction (24). Here, we show that miR-34b and miR-34c are downregulated in several brain areas with different degree of affectation in PD. Furthermore, we show compelling data suggesting that downregulation of these miRNAs affects key pathways in PD pathogenesis.

Two mechanisms have been described to control miR-34b/c expression. First, P53 activates miR-34b and miR-34c expression, cooperating in the control of cell proliferation and adhesion-independent growth (25) and inducing senescence (26). However, inhibition of P53 is unlikely to be the direct cause of miR-34b/c downregulation in PD, since P53 is found upregulated in autopsied PD brains (27), and several studies show that P53 activity is key in dopaminergic cell death (28). Secondly, miR-34b/c silencing is associated with CpG island hypermethylation in gastric, and colorectal cancers (19,29). Genes related to PD present abnormal methylation in some cancer types (30,31); however, a direct relation between epigenetics and neurodegeneration in PD has not been widely exploited yet. We could not detect significant hypermethylation of mir-34b/c promoter in PD samples, suggesting that this is not the main mechanism accounting for mir-34b/c downregulation. Additional studies are required

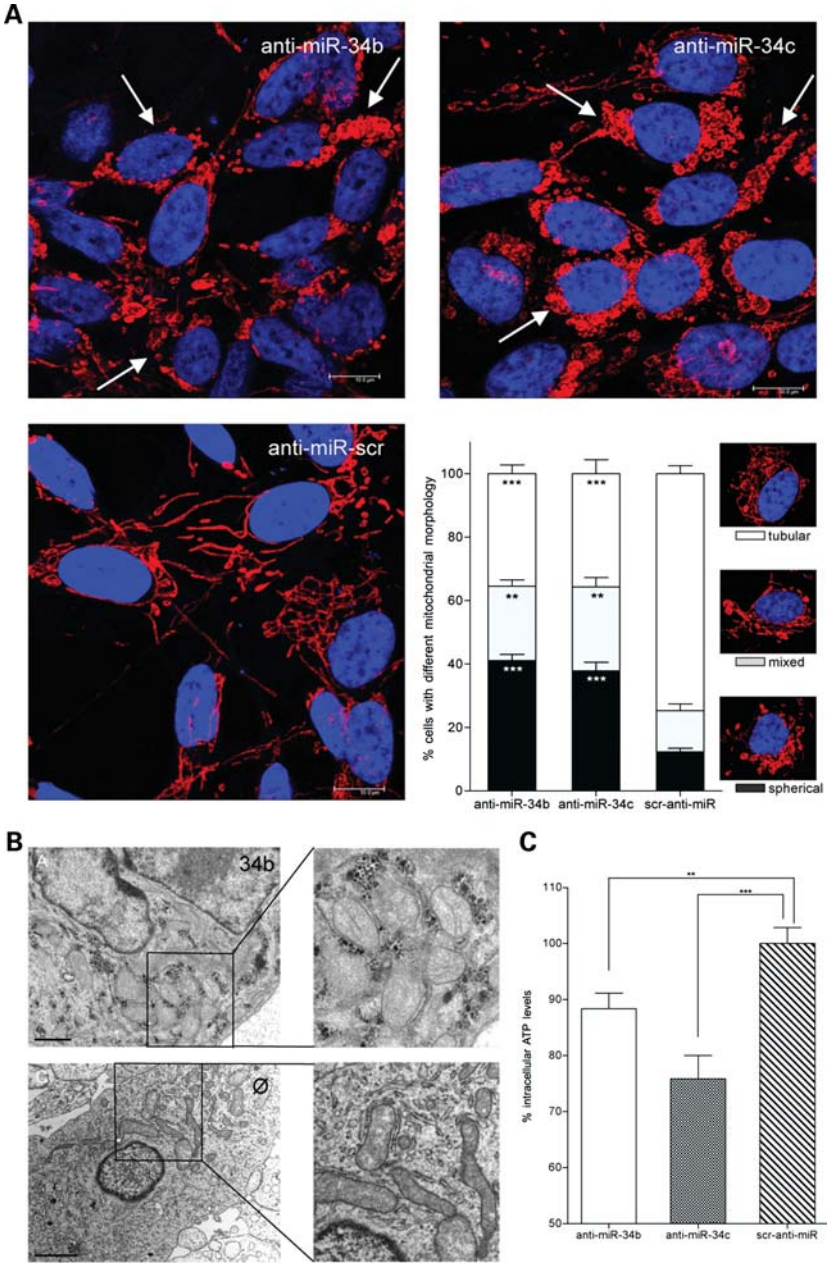


**Figure 4.** Mitochondrial morphology and intracellular ATP content after miR-34b or miR-34c depletion. (**A**) Citochrome-c immunostaining and DAPI staining of differentiated SH-SY5Y cells 48 h after transfection with either miR-34b (anti-miR-34b) or miR-34c (anti-miR-34c) inhibitors, or a scrambled-control sequence (scr-anti-miR). Plot shows the mean percentage of cells presenting tubular (white), spherical (black) and mixed (grey) mitochondrial morphology ± SEM ($n = 3$; $^{**}P < 0.01$; $^{***}P < 0.001$; using *t*-test). (**B**) Electron microscopy images showing mitochondrial ultrastructure in SH-SY5Y cells at 48 h after transfection with anti-miR-34b and in control non-transfected (*Ø*) SH-SY5Y cells. (**C**) Intracellular ATP levels 48 h upon transfection with either miR-34b (anti-miR-34b) or miR-34c (anti-miR-34c) inhibitors, or a scrambled sequence (scr-anti-miR); data are presented as the percentage (%) of ATP levels referred to the scr-anti-miR transfected control group ± SEM ($n = 3$; $^{**}P < 0.01$; $^{***}P < 0.001$, using *t*-test).

to address the mechanisms underlying miR-34b/c deregulation, including alterations in the pre-miRNA maturation process and/or miRNA stability.

We detected a significant decrease in the expression of mature miR-34b and miR-34c in the AM, SN, FC and in the CB of symptomatic PD patients. However, at clinical stages, Lewy inclusions are abundant in the AM and the SN, but mild or almost absent in the cortex and absent in the CB. Yet it is worth stressing that several functional abnormalities have been reported in the cortex of PD patients (32). For instance, mitochondrial complex I deficiency (33,34) and indices of OS have been detected in the cerebral cortex in PD (32). In addition, some PD-key proteins related to mitochondria, energy metabolism and OS responses are oxidativelly damaged (35), thus indicating impaired mitochondrial function and energy metabolism in the FC in the absence of LBs. Furthermore, abnormally phosphorylated SNCA and abnormally phosphorylated tau

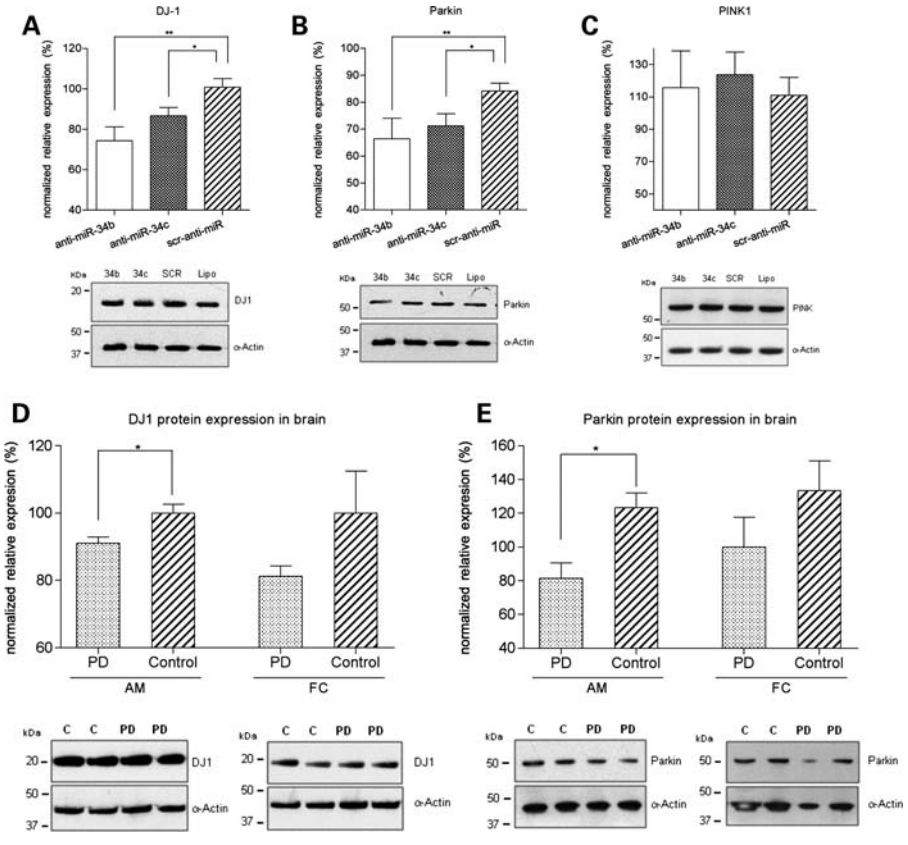


**Figure 5.** Expression of DJ1, Parkin and PINK1 in cells depleted of miR-34b or miR-34c, and in PD samples (listed in Supplementary Material, Table S2). (**A**–**C**) Protein levels of DJ1 (A), Parkin (B) and PINK1 (C) 48 h after transfection of either miR-34b (anti-miR-34b) or miR-34c (anti-miR-34c) inhibitors, or scrambled miRNA (scr-anti-miR). Expression of α-actin protein was used as a loading control. Cells treated with lipofectamine (lipo) were considered as the reference, for relative expression (%). Data are expressed as the percentage of expression with respect to lipofectamine treated control cells ± SEM ($n \geq 4$; $^{*}P < 0.05$; $^{**}P < 0.01$; *t*-test), and corresponding representative WBs are shown. (**D** and **E**) Levels of DJ1 (D) and Parkin (E) in control AM and FC, and symptomatic PD AM and FC. Expression levels were normalized with respect to α-actin expression. Data are expressed as the normalized relative expression ± SEM ($n = 4$; $^{*}P < 0.05$; using *t*-test), and corresponding representative WBs.

are found at the synaptic-enriched fractions of FC in PD (36). Recent observations have further demonstrated the presence of small abnormal aggregates of SNCA at the synapses (37,38). These are important independent observations showing that synaptic pathology occurs in the absence of LBs, and that a common alteration in the cerebral cortex in PD is pathology at the synapses rather than the presence of LBs. Although these aspects have not been studied in the CB, it is known that the cerebellothalamocortical pathway is altered in PD (39,40). Therefore, the present findings indicate a stronger relationship of miR-34b/c downregulation with complex molecular pathology in PD rather than with the mere distribution of LBs. Whether downregulation of miR-34b/c is a cause or a consequence of pathology remains to be elucidated. However, the present observations indicate that miR-34b/c downregulation occurs at early (pre-motor) stages of the disease (significantly decreased in AM, and reduced trend in the FC), thus suggesting a plausible role in the pathogenesis of PD. It is worth stressing that patients at pre-motor stages had not received any treatment related to PD, and therefore, miR-34b/c downregulation is not drug-related.

Impairment of mitochondrial function is central in the pathological process culminating in neuronal cell dysfunction in PD, occurring early in the course of the disease (41). Our data show compelling indications that a decrease in either miR-34b or miR-34c in differentiated neuronal cells compromises cell viability and mitochondrial function. These include a diminished capability of mitochondria to reduce MTT accompanied by a significant loss in the mitochondrial membrane potential, increased formation of ROS and decreased intracellular ATP levels. The loss of electrochemical gradient across the inner mitochondrial membrane may reflect a defect in the function of the mitochondrial complexes I–IV. However, we failed to detect changes in the expression levels of key components of different mitochondrial complexes. It remains to be elucidated whether miR-34b/c deficiency may induce changes in the expression and subsequent malfunction of other components of the mitochondrial complexes and/or proteins that modulate their activity. It is also plausible that miR-34b/c deregulation perturbs the expression of OS sensors, resulting in ROS production. This could contribute to sustained mitochondrial dysfunction, since mitochondria are particularly sensitive to ROS (33,42–44).

The expression and function of genes involved in recessive forms of familial PD, including *DJ1*, *PARKIN* and *PINK1*, are altered in idiopathic PD. For instance, the expression of *DJ1*, an OS sensor, is decreased in several brain areas (45) and cerebrospinal fluid (46) in sporadic PD cases. In addition, oxidized forms of DJ1, which may be dysfunctional, are increased in sporadic PD (47). Similarly, inactivation of Parkin, an E3 ubiquitin ligase, through nitrosative and oxidative stress may play a pathogenic role in sporadic PD (48). Importantly, our results show that miR-34b and miR-34c depletion in differentiated SH-SY5Y cells affects pathways that modulate Parkin and DJ1 dosage, resulting in moderately reduced levels of both proteins. Concordantly, PD brain samples presenting reduced expression of mir-34b/c also displayed a significant reduction in DJ1 and Parkin protein levels. Deficiency in either Parkin or DJ1 has been shown to be detrimental to cell survival, inducing mitochondrial dysfunction and oxidative damage (49–52). Altogether, these data suggest that miR-34b/c deficiency may cause mitochondrial dysfunction through a mechanism involving, at least, Parkin and DJ1 downregulation.

We have also demonstrated that miR-34b and miR-34c depletion in a neuroblastoma cell line results in significant alterations of mitochondrial morphology. Diseases of mitochondrial dysfunction that often have a neurodegenerative component present alterations in the dynamics of these organelles (53). In the case of PD, the interplay of PINK1 and Parkin dynamically regulates mitochondrial morphology (54–56). In addition, DJ1 depletion results in fragmented mitochondria, contributing to an increased sensitivity to OS (57). Therefore, the reduced levels of DJ1 and Parkin in cells depleted of miR-34b/c could contribute to the abnormal mitochondrial morphology.

In summary, we have shown that miR-34b/c downregulation is an early event in PD, and that miR-34b/c deregulation tags mitochondrial integrity and oxidative stress pathways, which are major hallmarks of PD. Mitochondrial protection and subsequent reduction in oxidative stress are important targets for prevention and long-term treatment of early stages of PD. Therefore, modulation of miR-34b/c dosage could be envisioned as an attractive target for neuroprotection-based therapeutic strategies.

## MATERIALS AND METHODS

### Patients

Brain samples were obtained from the Institute of Neuropathology Brain Bank following the guidelines of the local ethics committee. The time between death and brain processing named post-mortem time or post-mortem delay was between 3.00 and 11.00 h. Brains were removed from the skull and the left cerebral hemisphere, left cerebellum and alternate transversal sections of the brain stem were fixed in 4% buffered formalin. The rest of the brain and cerebellum was immediately cut into 1 cm thick coronal sections. These and the alternate sections of the brain stem were frozen on dry ice and stored at −80°C until use. Neuropathological studies were carried out on formalin-fixed paraffin embedded sections 4 μm thick of 25 standard selected areas which were processed for current neuropathological methods, including hematoxylin and eosin, Klüver-Barrera, and β-amyloid, hyper-phosphorylated tau, SNCA, ubiquitin, αB-crystalin, TDP-43 and astroglial and microglial immunohistochemistry.

PD-related pathology was graded following Braak stages (3,4). Cases with PD stages 4 and 5 (also named LBD stages 4 and 5) had suffered from parkinsonism and had been subjected to different treatments geared to control motor symptoms for variable period of time (cases 1–11, 18–19 and 21–23; Supplementary Material, Table S1); none of them had suffered from dementia. Cases with PD-related pathology stages 1–3 (LBD stages 1–3) had not suffered from motor symptoms, did not receive any specific therapy and the observation of LBs and LNs was an incidental feature at neuropathological examination (cases 12–17 and 20; Supplementary Material, Table S1). PD cases with additional pathology not related to synuclein, excepting those with a few neurofibrillary tangles in the entorhinal and transentorhinal cortices, were excluded from the study.

Age-matched control cases were chosen on the basis of the lack of neurological, metabolic and mental disorders, together with the lack of brain lesions including the absence of neurofibrillary tangles, SNCA inclusions, TDP-43 abnormalities and lack of small vascular disease after neuropathological examination following the same protocol as that used for PD cases. A few diffuse β-amyloid plaques and a few neurofibrillary tangles in the entorhinal cortex were the only abnormality in some cases.

Details regarding case information can be found in Supplementary Material, Table S1. For each sample, 50–60 mg of frozen tissue for every particular area was homogenized and then RNA isolated with miRNeasy (Qiagen) following manufacturer's instructions. RNA integrity was evaluated with Bioanalyzer 2100 (Applied Biosystems).

### Microarrays

MiRNA microarrays were performed by Exiqon, using mercury LNA microarrays (Sanger database v.8.1) where each individual PD AM sample was hybridized against a pool made of equitable quantities of all control AM samples.

### MiRNA rRT–PCR

MiRNA RT–PCR was performed using Taqman® miRNA-specific RT and rRT–PCR assays, following manufacturer's instructions in an AB 7900HT Fast Real-Time PCR System. For each region, all cases and controls were analyzed in the same rRT–PCR experiment, each sample was run in duplicates and the real-time reaction repeated at least twice. Relative quantification (RQ) as shown in graphs was calculated with the $-\triangle\triangle$Ct method (58) using U6B as a reference gene. RQ was calculated to compare expression values of both miR-34b and miR-34c normalized to that of U6B among PD and controls samples. These RQ and their statistical significance were obtained from a linear mixed effects model (59) that accounted for the different sources of variation derived from the experimental design (see supplementary methods for details).

### Cell lines and transfections

SH-SY5Y cells were grown in the Dulbecco's modified essential medium (DMEM) medium supplemented with 10% of inactivated fetal bovine serum (FBS) and kept in low pass (<15). Differentiation protocol consisted of 3 days RA 10 μM exposure, followed by 4 + 3 days of TPA 80 nM exposure, modified from ref. (20). HepG2 and h-TERT-RPE-1 (RPE-1) cells were grown in the DMEM medium supplemented with 10% of FBS and kept in low pass (<15).

Specific miRNA inhibitors for miR-34b, miR-34c and a scrambled sequence were purchased from both Dharmacon and Exiqon. For differentiated SH-SY5Y, cells were plated at day 3 of the differentiation process at 12 500 cells/ml and then transfected at day 10 with either one of the specific inhibitors or the scrambled sequence at 100 nM using Lipofectamine 2000™ (Invitrogen) according to the manufacturer's instructions. For transfection of undifferentiated SH-SY5Y, RPE-1 and HepG2 cells, the cells were plated 24 h prior to transfection at the following densities: 90 000, 50 000 and 40 000 cells/ml, respectively.

### MTT assays

Cells were transfected in 96 well plates in 12 independent experiments; then at 24, 48 and 72 h post-transfection, MTT was added to cell culture media at 0.5 mg/ml final concentration and incubated for 40 min at 37°C. Cells were lysed with 100 μl of dimethyl sulfoxide upon medium removal and absorbance was measured at 550 nm. In each experiment, determinations were performed in quintuplicate. Percentage of cell viability was calculated using absorbance values from cells transfected with the anti-scrambled sequence as a reference.

### ROS and mitochondrial membrane depolarization detection

Cells were plated for transfection in 24 MW plates over 13 mm cover slips, then at 24 and 48 h post-transfection they were incubated with either CM-$H_2$DCFDA ROS detection probes (Invitrogen) at 62.5 μg/μl or MitoTracker® Red CMXRos (Invitrogen) at 1 μM final concentration for 20 min at 37°C. Then cells were rinsed with PBS1X and fixed with 4% paraformaldehyde (4% PFA). Cover slips were mounted using Prolong with 4′,6-diamidino-2-phenylindole (DAPI) (Invitrogen) and images were taken with a Leica DM5000-CS confocal microscope. For quantification, three independent experiments were carried out and five fields were randomly captured for each condition and experiment. Around 400 cells were counted in each experiment. Statistical significance was calculated with two-tailed Student's *t*-test.

### Immunofluorescence

Cells were plated for transfection in 24 MW plates over 13 mm cover slips, then 48 and 72 h post-transfection cells were rinsed with PBS1X and fixed with 4% PFA. Cells were washed three times with PBS1X and permeabilized for 5 min in 0.1% Triton X-100 in PBS 1X (PBS-T). Cells were then incubated in blocking buffer (10% FBS, 0.1% PBS-T) for 1 h and then incubated with anti-cytochrome-c antibody from BD Bioscience (BD, 556432) for 2 h at room temperature (RT); cover slips were then rinsed with PBS-T and incubated with anti-rabbit Alexa Fluor 555 secondary antibody for 1 h at RT. Cover slips were mounted using Prolong with DAPI (Invitrogen). For quantification, three mitochondrial morphologies were considered: round, tubular and a mixed phenotype. Quantification was performed as previously indicated in three independent experiments.

### Electron microscopy

Cells were transfected in 6 MW plates, with either miR-34b or miR-34c inhibitors, or a scrambled sequence. Lipofectamine treated cells were used as an additional negative control. Cells were rinsed with PBS1X at 48 and 72 h after transfection. Cells were released from the plate with 700 μl of PB 0.1 M buffer per well by gentle scraping to produce a pellet cohesive enough to process after spinning at 800 g for 5 min. Supernatant was discarded and pellets were fixed with 2% PFA–2.5% glutaraldehyde in PB 0.1 M for 1 h at RT. The pellets were washed three times with PB 0.1 M and maintained in PFA 2% in PB 0.1 M and then post-fixed by immersion in 1% osmium tetraoxide, embedded in EPON-812 and cut with an ultramicrotome. Ultrathin sections were stained with toluidine blue and finally selected sections were collected in copper grids, stained with uranyl acetate and Reynold's lead citrate. Sections were directly visualized with a Jem-1011 transmission electron microscope (Jeol).

### ATP content determination

Cells were transfected in quintuplicate in 96 MW plates, with either miR-34b, miR-34c inhibitors or a scrambled sequence. Lipofectamine treated cells were used as an additional negative control. Cellular ATP levels were quantified at 48 and 72 h after transfection using a luciferin/luciferase based assay. Cells were lysed with 100 μl of ATP lysis buffer previously reported (62), and both protein and ATP levels were assessed in triplicate. Protein was determined using the bicinchoninic acid assay (Pierce). ATP was determined using an ATP determination kit (Invitrogen, molecular probes A22066) according to the manufacturer's instructions. ATP levels (nM) were normalized to the protein levels in each sample. ATP levels for each condition were referred to the mean ATP content in cells transfected with the scrambled-control sequence. Statistical significance was calculated with two-tailed Student's *t*-test.

### Protein extraction and western blot analysis

Cells were rinsed with PBS1X, lysed with 0.05% SDS, boiled for 2 min and centrifuged at 10 000*g* and 4°C for 10 min. The supernatant was diluted with 6× Laemmli loading buffer and boiled for 2 min prior to loading. Proteins were resolved by 10% sodium dodecyl sulfate–polyacrilamide gel electrophoresis, and electroblotted onto nitrocellulose membranes using the i-Blot dry transfer system (Invitrogen). Membranes were blocked with blocking solution (3% BSA, 0.1% Tween-20, TBS1X) for at least 1 h at RT. Primary antibodies were

incubated overnight at 4°C, then membranes were washed with TBS-0.1% Tween and incubated for 1 h at RT with secondary antibodies (DakoCytomation) at a dilution of 1:2 000. After washing, membranes were developed with the enhanced chemiluminiscence system (ECL, Amersham Life Sciences). Western blot signal was quantified using ImageJ software. Expression of α-actin was used as a loading normalization control. The following primary antibodies were used: mouse monoclonal anti-α-Actin (MAB1501, Chemicon); mouse monoclonal anti-Caspase 9 (9508, Cell Signalling); purified mouse anti-human PARP (51-6639GR, BD); rabbit polyclonal anti-DJ1 (ab18257, Abcam); rabbit polyclonal anti-Parkin (ab15954, Abcam); rabbit polyclonal anti-PINK1 (ab23707, Abcam); and MitoProfile® total OXPHOS human antibody cocktail (MS601, Mitoscience).

## SUPPLEMENTARY MATERIAL

Supplementary Material is available at *HMG* online.

*Conflict of Interest statement*. None declared.

## FUNDING

This work was supported by the Spanish Ministry of Health 'Fondo de Investigaciones Sanitarias' (PI081367); the Sixth Framework Programme of the European Commission through the SIROCCO integrated project LSHG-CT-2006-037900; the Spanish Ministry of Science and Innovation (SAF2008-00357); the Generalitat of Catalonia (Department of Health and Department of Economy and knowledge); the Spanish Ministry of Health: 'Programa Miguel Servet' (E.M.). Instituto de Salud Carlos III: 'Contrato Postdoctoral Sara Borrell' (S.P.) and BEFI contract (E.M.-M.).

## REFERENCES

1. de Rijk, M.C., Launer, L.J., Berger, K., Breteler, M.M., Dartigues, J.F., Baldereschi, M., Fratiglioni, L., Lobo, A., Martinez-Lage, J., Trenkwalder, C. *et al.* (2000) Prevalence of Parkinson's disease in Europe: a collaborative study of population-based cohorts. *Neurology*, **54**, S21–S23.
2. Shulman, J.M., De Jager, P.L. and Feany, M.B. (2010) Parkinson's disease: genetics and pathogenesis. *Annu. Rev. Pathol.*, [Epub ahead of print].
3. Braak, H., Del Tredici, K., Rüb, U., de Vos, R.A., Jansen Steur, E.N. and Braak, E. (2003) Staging of brain pathology related to sporadic Parkinson's disease. *Neurobiol. Aging*, **24**, 197–211.
4. Braak, H., Ghebremedhin, E., Rüb, U., Bratzke, H. and Del Tredici, K. (2004) Stages in the development of Parkinson's disease-related pathology. *Cell Tissue Res.*, **318**, 121–134.
5. Dauer, W. and Przedborski, S. (2003) Parkinson's disease: mechanisms and models. *Neuron*, **39**, 889–909.
6. Jellinger, K.A. (2004) Lewy body-related alpha-synucleinopathy in the aged human brain. *J. Neural. Transm.*, **111**, 1219–1235.
7. Saito, Y., Ruberu, N.N., Sawabe, M., Arai, T., Kazama, H., Hosoi, T., Yamanouchi, H. and Murayama, S. (2004) Lewy body-related alpha-synucleinopathy in aging. *J. Neuropathol. Exp. Neurol.*, **63**, 742–749.
8. Douglas, M.R., Lewthwaite, A.J. and Nicholl, D.J. (2007) Genetics of Parkinson's disease and parkinsonism. *Expert Rev. Neurother.*, **7**, 657–666.
9. Tan, E.K. and Skipper, L.M. (2007) Pathogenic mutations in Parkinson disease. *Hum. Mutat.*, **28**, 641–653.
10. Xiromerisiou, G., Dardiotis, E., Tsimourtou, V., Kountra, P.M., Paterakis, K.N., Kapsalaki, E.Z., Fountas, K.N. and Hadjigeorgiou, G.M. (2010) Genetic basis of Parkinson's disease. *Neurosurg. Focus*, **28**, E7.
11. Gao, F.B. (2008) Posttranscriptional control of neuronal development by miRNA networks. *Trends Neurosci.*, **31**, 20–26.
12. Schratt, G. (2009) microRNAs at the synapse. *Nat. Rev. Neurosci.*, **10**, 842–849.
13. Brodersen, P. and Voinnet, O. (2009) Revisiting the principles of microRNA target recognition and mode of action. *Nat. Rev. Mol. Cell Biol.*, **10**, 141–148.
14. Ghildiyal, M. and Zamore, P.D. (2009) Small silencing RNAs: an expanding universe. *Nat. Rev. Genet.*, **10**, 94–108.
15. Sonntag, K.C. (2010) MicroRNAs and deregulated gene expression networks in neurodegeneration. *Brain Res.*, **1338**, 48–57.
16. Kim, J., Inoue, K., Ishii, J., Vanti, W.B., Voronov, S.V., Murchison, E., Hannon, G. and Abeliovich, A. (2007) A microRNA feedback circuit in midbrain dopamine neurons. *Science*, **317**, 1220–1224.
17. Wang, G., van der Walt, J.M., Mayhew, G., Li, Y.J., Züchner, S., Scott, W.K., Martin, E.R. and Vance, J.M. (2008) Variation in the miRNA binding site of FGF20 confers risk for Parkinson disease by overexpression of α-synuclein. *Am. J. Hum. Genet.*, **82**, 283–289.
18. Junn, E., Lee, K.W., Jeong, B.S., Chan, T.W., Im, J.Y. and Mouradian, M.M. (2007) Repression of α-synuclein expression and toxicity by microRNA-7. *Proc. Natl Acad. Sci. USA*, **106**, 13052–13057.
19. Toyota, M., Suzuki, H., Sasaki, Y., Maruyama, R., Imai, K., Shinomura, Y. and Tokino, T. (2008) Epigenetic silencing of microRNA-34b/c and B-cell translocation gene 4 is associated with CpG island methylation in colorectal cancer. *Cancer Res.*, **68**, 4123–4132.
20. Presgraves, S.P., Ahmed, T., Borwege, S. and Joyce, J.N. (2004) Terminally differentiated SH-SY5Y cells provide a model system for studying neuroprotective effects of dopamine agonists. *Neurotox. Res.*, **5**, 579–598.
21. Dodson, M.W. and Guo, M. (2007) Pink1, Parkin, DJ-1 and mitochondrial dysfunction in Parkinson's disease. *Curr. Opin. Neurobiol.*, **17**, 331–337.
22. Martinat, C., Shendelman, S., Jonason, A., Leete, T., Beal, M.F. *et al.* (2004) Sensitivity to oxidative stress in DJ-1-deficient dopamine neurons: an ES- derived cell model of primary Parkinsonism. *PLoS Biol.*, **2**, e327.
23. Taira, T., Saito, Y., Niki, T., Iguchi-Ariga, S.M., Takahashi, K. and Ariga, H. (2004) DJ-1 has a role in antioxidative stress to prevent cell death. *EMBO Rep.*, **5**, 213–218.
24. Eacker, S.M., Dawson, T.M. and Dawson, V.L. (2009) Understanding microRNAs in neurodegeneration. *Nat. Rev. Neurosci.*, **10**, 837–841.
25. Corney, D.C., Flesken-Nikitin, A., Godwin, A.K., Wang, W. and Nikitin, A.Y. (2007) MicroRNA-34b and MicroRNA-34c are targets of p53 and cooperate in control of cell proliferation and adhesion-independent growth. *Cancer Res.*, **67**, 8433–8438.
26. Kumamoto, K., Spillare, E.A., Fujita, K., Horikawa, I., Yamashita, T., Appella, E., Nagashima, M., Takenoshita, S., Yokota, J. and Harris, C.C. (2008) Nutlin-3a activates p53 to both down-regulate inhibitor of growth 2 and up-regulate mir-34a, mir-34b, and mir-34c expression, and induce senescence. *Cancer Res.*, **68**, 3193–3203.
27. Mogi, M., Kondo, T., Mizuno, Y. and Nagatsu, T. (2007) p53 protein, interferon-γ, and NF-κB levels are elevated in the parkinsonian brain. *Neurosci. Lett.*, **414**, 94–97.
28. da Costa, C.A. and Checler, F. (2010) Apoptosis in Parkinson's disease: is p53 the missing link between genetic and sporadic Parkinsonism? *Cell Signal.*, [Epub ahead of print].
29. Suzuki, H., Yamamoto, E., Nojima, M., Kai, M., Yamano, H.O., Yoshikawa, K., Kimura, T., Kudo, T., Harada, E., Sugai, T. *et al.* (2010) Methylation-associated silencing of microRNA-34b/c in gastric cancer and its involvement in an epigenetic field defect. *Carcinogenesis*, **31**, 2066–2073.
30. Liu, H., Liu, W., Wu, Y., Zhou, Y., Xue, R., Luo, C., Wang, L., Zhao, W., Jiang, J.D. and Liu, J. (2005) Loss of epigenetic control of synuclein-{gamma} gene as a molecular indicator of metastasis in a wide range of human cancers. *Cancer Res.*, **65**, 7635–7643.
31. Zhao, W., Liu, H., Liu, W., Wu, Y., Chen, W., Jiang, B., Zhou, Y., Xue, R., Luo, C., Wang, L. *et al.* (2006) Abnormal activation of the synuclein-gamma gene in hepatocellular carcinomas by epigenetic alteration. *Int. J. Oncol.*, **28**, 1081–1088.
32. Dexter, D.T., Sian, J., Rose, S., Hindmarsh, J.G., Mann, V.M., Cooper, J.M., Wells, F.R., Daniel, S.E., Lees, A.J., Schapira, A.H. *et al.* (1994)

Indices of oxidative stress and mitochondrial function in individuals with incidental Lewy body disease. *Ann. Neurol.*, **35**, 38–44.
33. Navarro, A., Boveris, A., Bández, M.J., Sánchez-Pino, M.J., Gómez, C., Muntané, G. and Ferrer, I. (2009) Human brain cortex: mitochondrial oxidative damage and adaptive response in Parkinson disease and in dementia with Lewy bodies. *Free Radic. Biol. Med*, **46**, 1574–1580.
34. Parker, W.D.J., Parks, J.K. and Swerdlow, R.H. (2008) Complex I deficiency in Parkinson's disease frontal cortex. *Brain Res.*, **1189**, 215–218.
35. Ferrer, I. (2009) Early involvement of the cerebral cortex in Parkinson's disease: convergence of multiple metabolic defects. *Prog. Neurobiol.*, **88**, 89–103.
36. Muntané, G., Martínez, A. and Ferrer, I. (2008) Phosphorylation of tau and alphasynuclein in synaptic-enriched fractions of the frontal cortex in Alzheimer's disease and related alpha-synucleinopathies. *Neuroscience*, **152**, 913–923.
37. Schulz-Schaeffer, W.J. (2010) The synaptic pathology of alpha-synuclein aggregation in dementia with Lewy bodies, Parkinson's disease and Parkinson's disease with dementia. *Acta Neuropathol.*, **120**, 131–143.
38. Tanji, M.F., Mimura, J., Itoh, K., Takahashi, H. and Wakabayashi, K. (2010) Proteinase K-resistant alpha-synuclein is deposited in presynapses in human Lewy body disease and A53T alpha-synuclein transgenic mice. *Acta Neuropathol.*, **120**, 145–154.
39. Ni, Z., Pinto, A.D., Lang, A.E. and Chen, R. (2010) Involvement of the cerebellothalamocortical pathway in Parkinson disease. *Ann. Neurol.*, **68**, 816–824.
40. Payoux, P., Brefel-Courbon, C., Ory-Magne, F., Regragui, W. and Thalamas, C. (2010) Motor activation in multiple system atrophy and Parkinson's disease: a PET study. *Neurology*, **75**, 1174–1180.
41. Winklhofer, K.F. and Haass, C. (2010) Mitochondrial dysfunction in Parkinson's disease. *Biochim. Biophys. Acta*, **1802**, 29–44.
42. Schapira, A.H., Cooper, J.M., Dexter, D., Clark, J.B., Jenner, P. *et al.* (1990) Mitochondrial complex I deficiency in Parkinson's disease. *J. Neurochem.*, **54**, 823–827.
43. Schapira, A.H. (2008) Mitochondria in the aetiology and pathogenesis of Parkinson's disease. *Lancet Neurol.*, **7**, 97–109.
44. Schapira, A.H., Mann, V.M., Cooper, J.M., Dexter, D., Daniel, S.E., Jenner, P., Clark, J.B. and Marsden, C.D. (1990) Anatomic and disease specificity of NADH CoQ1 reductase (complex I) deficiency in Parkinson's disease. *J. Neurochem.*, **55**, 2142–2145.
45. Kumaran, R., Vandrovcova, J., Luk, C., Sharma, S., Renton, A., Wood, N.W., Hardy, J.A., Lees, A.J. and Bandopadhyay, R. (2009) Differential DJ-1 gene expression in Parkinson's disease. *Neurobiol. Dis.*, **36**, 393–400.
46. Foulds, P., Mann, D.M., Mitchell, J.D. and Allsop, D. (2010) Parkinson disease: progress towards a molecular biomarker for Parkinson disease. *Nat. Rev. Neurol.*, **6**, 359–361.
47. Choi, J., Sullards, M.C., Olzmann, J.A., Rees, H.D., Weintraub, S.T. *et al.* (2006) Oxidative damage of DJ-1 is linked to sporadic Parkinson and Alzheimer diseases. *J. Biol. Chem.*, **281**, 10816–10824.
48. Dawson, T.M. and Dawson, V.L. (2010) The role of Parkin in familial and sporadic Parkinson's disease. *Mov. Disord.*, **25**, S32–S39.
49. Greene, J.C., Whitworth, A.J., Kuo, I., Andrews, L.A., Feany, M.B. and Pallanck, L.J. (2003) Mitochondrial pathology and apoptotic muscle degeneration in Drosophila parkin mutants. *Proc. Natl Acad. Sci. USA*, **100**, 4078–4083.
50. Irrcher, I., Aleyasin, H., Seifert, E.L., Hewitt, S.J., Chhabra, S., Phillips, M., Lutz, A.K., Rousseaux, M.W., Bevilacqua, L., Jahani-Asl, A. *et al.* (2010) Loss of the Parkinson's disease-linked gene DJ-1 perturbs mitochondrial dynamics. *Hum. Mol. Genet.*, **19**, 3734–3746.
51. Palacino, J.J., Sagi, D., Goldberg, M.S., Krauss, S., Motz, C., Wacker, M., Klose, J. and Shen, J. (2004) Mitochondrial dysfuncion and oxidative damage in Parkin-deficient mice. *J. Biol. Chem.*, **279**, 18614–18622.
52. Pesah, Y., Pham, T., Burgess, H., Middlebrooks, B., Verstreken, P., Zhou, Y., Harding, M., Bellen, H. and Mardon, G. (2004) Drosophila parkin mutants have decreased mass and cell size and increased sensitivity to oxygen radical stress. *Development*, **131**, 2183–2194.
53. Chen, H. and Chan, D.C. (2009) Mitochondrial dynamics—fusion, fission, movement, and mitophagy—in neurodegenerative diseases. *Hum. Mol. Genet.*, **18**, R169–R176.
54. Clark, I.E., Dodson, M.W., Jiang, C., Cao, J.H., Huh, J.R., Seol, J.H., Yoo, S.J., Hay, B.A. and Guo, M. (2006) Drosophila pink1 is required for mitochondrial function and interacts genetically with parkin. *Nature*, **441**, 1162–1166.
55. Deng, H., Dodson, M.W., Huang, H. and Guo, M. (2008) The Parkinson's disease genes pink1 and parkin promote mitochondrial fission and/or inhibit fusion in Drosophila. *Proc. Natl Acad. Sci. USA*, **105**, 14503–14508.
56. Poole, A.C., Thomas, R.E., Andrews, L.A., McBride, H.M., Whitworth, A.J. and Pallanck, L.J. (2008) The PINK1/Parkin pathway regulates mitochondrial morphology. *Proc. Natl Acad. Sci. USA*, **105**, 1638–1643.
57. Irrcher, I., Aleyasin, H., Seifert, E.L., Hewitt, S.J., Chhabra, S., Phillips, M., Lutz, A.K., Rousseaux, M.W., Bevilacqua, L., Jahani-Asl, A. *et al.* (2010) Loss of the Parkinson's disease-linked gene DJ-1 perturbs mitochondrial dynamics. *Hum. Mol. Genet.*, **19**, 3734–3746.
58. Livak, K.J. and Schmittgen, T.D. (2001) Analysis of relative gene expression data using real-time quantitative PCR and the 2 -△△Ct method. *Methods*, **25**, 402–408.
59. Steibel, J., Poletto, R., Coussens, P.M. and Rosa, G.J.M. (2009) A powerful and flexible linear mixed model framework for the analysis of relative quantification RT-PCR data. *Genomics*, **94**, 146–152.
60. Lujambio, A., Calin, G.A., Villanueva, A., Ropero, S., Sánchez-Céspedes, M., Blanco, D., Montuenga, L.M., Rossi, S., Nicoloso, M.S., Faller, W.J. *et al.* (2008) A microRNA DNA methylation signature for human cancer metastasis. *Proc. Natl Acad. Sci.*, **105**, 13556–13561.
61. Lewin, J., Schmitt, A., Adorján, P., Hildmann, T. and Piepenbrock, C. (2004) Quantitative DNA methylation analysis based on four-dye trace data from direct sequencing of PCR amplificates. *Bioinformatics*, **20**, 3005–3012.
62. Wang, X., Dykens, J.A., Perez, E., Liu, R., Yang, S., Covey, D.F. and Simpkins, J.W. (2006) Neuroprotective effects of 17beta-estradiol and nonfeminizing estrogens against H2O2 toxicity in human neuroblastoma SK-N-SH cells. *Mol. Pharmacol.*, **70**, 395–404.